Widespread rifting and retreat of ice-shelf margins in the eastern Amundsen Sea Embayment between 1972 and 2011

Joseph A. MacGREGOR,[1] Ginny A. CATANIA,[1,2] Michael S. MARKOWSKI,[1] Alan G. ANDREWS[1]

[1]*Institute for Geophysics, University of Texas at Austin, Austin, TX, USA*
E-mail: joemac@ig.utexas.edu
[2]*Department of Geological Sciences, University of Texas at Austin, Austin, TX, USA*

ABSTRACT. The major outlet glaciers that drain the eastern sector of the Amundsen Sea Embayment (Smith, Haynes, Thwaites and Pine Island) are among the largest, fastest-flowing and fastest-thinning glaciers in West Antarctica. Their recent ice-flow acceleration is linked to ocean-induced ice-shelf thinning, but may also arise from additional losses of ice-shelf buttressing that are not well understood. Here we present a comprehensive history of coastal change in the eastern Amundsen Sea Embayment between 1972 and 2011 derived mostly from Landsat imagery. The termini of all four major outlet glaciers have retreated, but retreat is most rapid along the ice-shelf margins, where progressive rifting has occurred. This pattern of retreat coincides with the recent acceleration of grounded ice and contributed to loss of ice-shelf buttressing. The observed pattern of margin-led gradual ice-shelf disintegration appears to be common in accelerating ocean-terminating outlet glaciers. We hypothesize that this pattern is part of a positive feedback between glacier acceleration and rift growth that could drive further buttressing loss in the eastern Amundsen Sea Embayment.

INTRODUCTION

The West Antarctic ice sheet is presently in a state of negative mass balance (Chen and others, 2009) due largely to the eastern sector of the Amundsen Sea Embayment (ASE), which contains four major outlet glaciers (Smith, Haynes, Thwaites and Pine Island) that are accelerating (Rignot, 2001, 2006, 2008; Joughin and others, 2003, 2010) and thinning rapidly (e.g. Shepherd and others, 2002; Thomas and others, 2004a; Pritchard and others, 2009). Understanding the mechanisms behind glacier acceleration in the ASE provides critical context for predictions of its future evolution (Lemke and others, 2007). Further thinning of the floating extensions of these glaciers or other changes that reduce buttressing (e.g. rifting) could lead to additional acceleration of grounded ice (Schmeltz and others, 2002; Joughin and others, 2010) and grounding-line retreat (e.g. Rignot, 2001). The latter is of particular concern because of the landward-sloping topography beneath these marine-based glaciers (Holt and others, 2006; Vaughan and others, 2006) rendering them dynamically unstable if grounding-line retreat continues (Schoof, 2007).

The amount of buttressing that an ice shelf or tongue provides to upstream grounded ice depends on how much shear is generated along its margins (bay walls or adjacent slower-flowing ice) and/or areas of localized grounding (e.g. ice rises), representing lateral and basal drag, respectively. These drags are functions of both contact area and friction. Enhanced delivery of Circumpolar Deep Water into the eastern Amundsen Sea over the last two decades has increased melt rates beneath Pine Island Glacier's ice shelf (Jacobs and others, 2011). The resultant ice-shelf thinning has reduced both lateral and basal drag there and likely initiated its recent acceleration (Rignot, 2002; Jenkins and others, 2010); this process also appears to have affected the eastern ASE's other outlet glaciers (Schmeltz and others, 2001).

While previous studies reported other changes in the ASE's floating ice (e.g. increased rifting) that broadly suggest additional loss of lateral drag between 1972 and 2002 (Bindschadler, 2002; Swithinbank and others, 2003), these studies are limited either spatially or temporally. To understand better the evolution of ice-shelf buttressing in the eastern ASE, here we comprehensively document the satellite history of coastal change in the eastern ASE since 1972 and evaluate this coastal change in terms of reported glacier accelerations.

DATA AND METHODS
Satellite data and coastline tracing

We compiled 158 Landsat scenes acquired over the eastern ASE between December 1972 and November 2011, some of which have been used in previous studies of coastal change in the eastern ASE (e.g. Bindschadler, 2002; Rignot, 2002; Swithinbank and others, 2003, 2004). We separated these scenes by calendar year by dividing each austral summer into two periods across 1 January of each year. Using this approach we generated 44 mosaics and, where sufficient Landsat coverage was available, we produced multiple mosaics for a single period of the austral summer either before or after 1 January. We also compiled 38 European Remote-sensing Satellite (ERS) synthetic aperture radar (SAR) scenes available within our study area that were chosen to fill gaps in Landsat coverage of the ASE coastline between 1992 and 1998. From these scenes, we produced seven additional mosaics and analyzed them in the same manner as for the Landsat scenes. Available imagery is sparse before 1994 but available for every year thereafter. For Pine Island Glacier only, we include older coastline positions derived from 1947 and 1966 aerial photography (Rignot, 2002) and 1963 satellite photography (Kim and others, 2007).

The available Landsat scenes were corrected radiometrically and geometrically (level 1G); Landsat-7 scenes (1997–2011) were also orthorectified (level 1Gt). No additional radiometric corrections were applied, nor was any
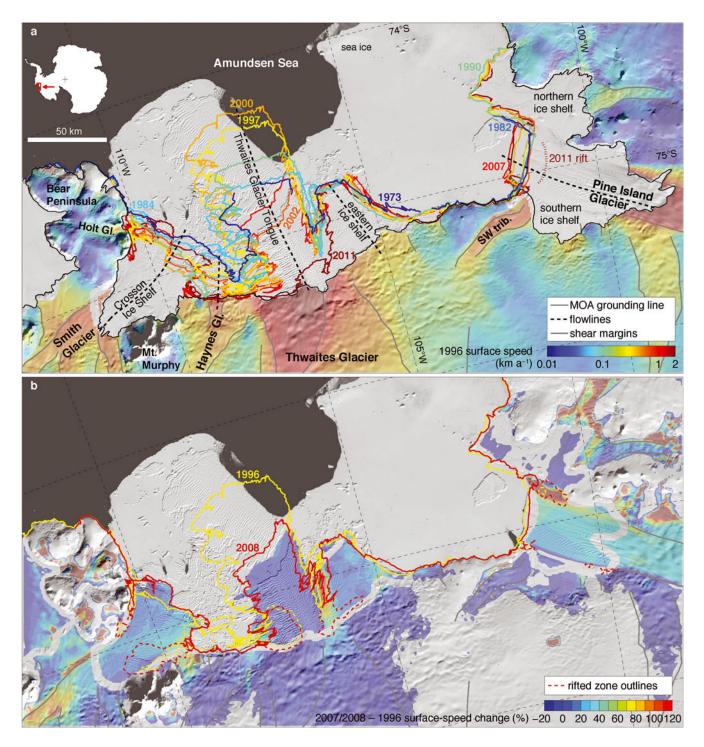
Fig. 1. (a) Evolution of the eastern ASE coastline between 1972 and 2011. Grayscale background is 2003–04 Mosaic of Antarctica (MOA). Superimposed coastlines are traced Landsat-1 through -7 imagery. For clarity, only nine out of 51 coastlines traced in this study are shown; Animations 1–4 show the complete coastline history. 1996 surface velocities (Joughin and others, 2009) are shown only for ice upstream of the 2003–04 MOA grounding line (Scambos and others, 2007). Shear margins on grounded ice were traced along coherent maxima in the absolute value of the lateral shear strain rate derived from the 1996 surface velocities. Key central flowlines are shown for the five major ice shelves and tongues in the eastern ASE. Inset map shows the location of the study area in Antarctica. (b) Percent change in surface speed between 1996 (Joughin and others, 2009) and 2007–08 (Rignot and others, 2011). The two coastlines bounding this period (1996 and 2008) are also shown, along with outlines of rifted zones at those times. The missing data across the grounding zone are due to missing 1996 surface speeds there. Note that the color scales are saturated to better illustrate the spatial variation of speed change and that portions of some slower-flowing regions (<50 m a^{-1}; e.g. Bear Peninsula) show large relative speed changes that are likely spurious.

contrast stretching necessary for image analysis. The spatio-temporal resolution of available digital elevation models (DEMs) and recent rapid thinning of eastern ASE outlet glaciers (e.g. Pritchard and others, 2009) limit the geodetic accuracy of these scenes. Our study is focused on floating ice, where surface slopes outside of crevasses/rifts are low,

so inconsistent orthorectification introduces limited geodetic uncertainty.

We then traced the coastline in these Landsat and ERS SAR mosaics manually at a scale of 1 : 50 000 (Figs 1 and 2; Table 1; Animations 1–4). The spatial resolution of Landsat sensors improved over time from 60 m to 15 m. Although
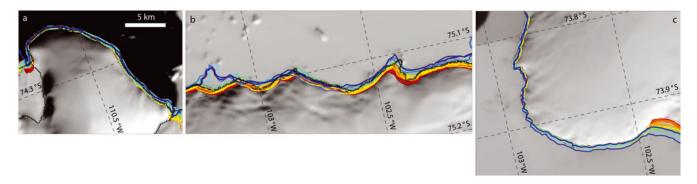
Fig. 2. Coastlines along portions of the eastern ASE coastline that were mostly stable between 1972 and 2011. (a) Bear Peninsula; (b) the coastline between Thwaites and Pine Island Glaciers; (c) Canisteo Peninsula. The coastlines of all 51 Landsat and ERS SAR mosaics are shown. The format of these maps and the coastline color scale are the same as for Figure 1 and the scale is the same for all three panels.

other later sensors often have finer resolution, a resolution of 30–60 m is sufficient to distinguish the calving front and/or rifts, and our Landsat-derived coastline traces agree well with contemporaneous traces derived from ERS SAR. For Landsat, we found that coastlines were often simplest to trace in color-infrared mode. An advantage of this approach is that color differences can be used to better distinguish floating ice masses attached to grounded ice from the ice melange or sea water visible inside rifts. A potential drawback is that for Landsat-7 (1999–present) we did not use the 15 m resolution panchromatic band 8. However, we found that delineation of the coastline was unaffected by the use of 30 m resolution data for the bands that form a colour-infrared image.

Where possible, we co-registered older scenes with newer ones using rock outcrops and slower-flowing portions of the coastline that either remained stationary or changed slowly throughout our study period (Fig. 2). We then adjusted the coastlines traced in the mosaicked imagery to produce the best possible co-alignment in these regions. With this approach, geodetic accuracy does not necessarily improve, but the relative positioning uncertainty between traced coastlines decreases significantly, as evidenced by the steady terminus advances (linear over time) that we measured along the central flowlines of the outlet glaciers (Fig. 3). These adjustments generally decreased over time as the georeferencing of satellite imagery either improved or became more self-consistent. No adjustments were made to scenes collected after 1997, but some 1972 scenes required adjustments of >20 km. Based on the residual mismatch between traces in regions that have a quasi-stable coastline (Fig. 2), we estimate our relative positioning uncertainty to be <0.5 km. The mean range of acquisition dates for the scenes that formed each Landsat mosaic is 15 days. For the maximum ice-flow speeds in this region ($\sim$4 km a^{-1} on Pine Island Glacier in 2010), that mean date range is equivalent to a relative positioning uncertainty of <0.2 km.

Along-flow terminus histories

From the imagery compilation and coastline tracing, we identified the terminus position through time along central

Table 1. Descriptions of online animations of coastline history and rifting evolution. Full animations available at www.igsoc.org/hyperlink
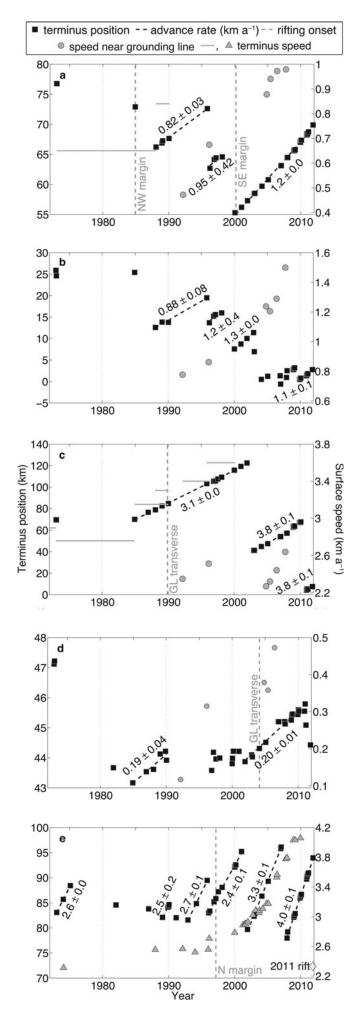
Animation number	Description
1	Complete history of coastlines between 1972 and 2011 traced in this study. Grayscale background is MOA and shows the eastern ASE region expanded from Figure 1. Mean date of each mosaic is shown for each coastline/frame. Traced coastlines are shown using same color scale as for Figure 1, along with outlines of the detached former Thwaites Glacier Tongue (sometimes referred to as the Thwaites Iceberg Tongue, e.g. Ferrigno and others, 1993). Full animation available at http://www.igsoc.org/hyperlink/11J262_Animation1.mov
2	Coastline history of Crosson Ice Shelf between 1972 and 2011. Same format as Animation 1. Full animation available at http://www.igsoc.org/hyperlink/11J262_Animation2.mov
3	Coastline history of the grounding-line region of Thwaites Glacier Tongue and the eastern ice shelf. Same format as Animation 1. Full animation available at http://www.igsoc.org/hyperlink/11J262_Animation3.mov
4	Coastline history of Pine Island Glacier between 1972 and 2011. Same format as Animation 1. Full animation available at http://www.igsoc.org/hyperlink/11J262_Animation4.mov
5	Selected Landsat mosaics of Crosson Ice Shelf between 1972 and 2011. Region shown is similar to Animation 2. Year of mosaic is given in lower right-hand corner. Traced coastline is shown in red. Full animation available at http://www.igsoc.org/hyperlink/11J262_Animation5.mov
6	Selected Landsat mosaics of the grounding-line region of Thwaites Glacier Tongue and the eastern ice shelf. Region shown is similar to Animation 3, but centered $\sim$10 km to the southwest to highlight the grounding-line region. Same format as Animation 5. Full animation available at http://www.igsoc.org/hyperlink/11J262_Animation6.mov
7	Selected Landsat mosaics of Pine Island Glacier's terminus. Region shown is similar to Animation 4, but centered $\sim$25 km to the east–southeast to highlight the northern shear margin of the ice shelf. Same format as Animation 5. Full animation available at http://www.igsoc.org/hyperlink/11J262_Animation7.mov

flowlines of the eastern ASE's four major outlet glaciers (Fig. 3). Flowlines were calculated using 1996 surface velocities derived from interferometric SAR (InSAR) and speckle tracking (Joughin and others, 2009). Where those velocity data end, either at or upstream of the 1996 terminus, the flowline is extended along the last measured velocity azimuth. Terminus position along a flowline is the linearly interpolated intersection of the flowline with the traced coastline. Flowlines were chosen based on both the coverage of the 1996 surface velocity map and our goal of intersecting the maximum possible number of traced coastlines.

We evaluated two different methods for calculating terminus position over time. In the first method, we calculated the intersection of each flowline/coastline pair by linearly interpolating each vector defined by two consecutive flowline points and determining whether it intersected the equivalent linear interpolation of any two consecutive coastline points. The flowlines are smoothly varying, whereas the coastlines were manually traced with the assumption that the coastline is a straight line between individual points (mean distance between points of 206 m). In heavily rifted regions where the coastline is not smoothly varying, this assumption may break down.

The second method follows Moon and Joughin (2008) who tracked the change in area of an open-ended box, the downstream end of which is the glacier terminus and the across-flow width of which is the majority of the glacier width. They argued that this 'box' method better accounts for terminus position changes than a single flowline. Because the width of most of the ice shelves in the eastern ASE is much larger than that of many of the Greenland outlet glaciers that Moon and Joughin (2008) studied, and because of the non-uniform ice-shelf marginal retreat that we observed (e.g. Fig. 1), we tested the box method across Pine Island Glacier only (Fig. 4). It is easiest to interpret such a record for Pine Island Glacier because of its relatively simple terminus shape and we used a 21.5 km wide box that includes about two-thirds of the near-terminus width of the glacier.

Fig. 3. Histories of terminus position and surface speed along flowlines of the eastern ASE's major outlet glaciers between 1972 and 2011. (a) Smith Glacier/Crosson Ice Shelf; (b) Haynes Glacier; (c) Thwaites Glacier Tongue; (d) Thwaites Glacier's eastern ice shelf; (e) Pine Island Glacier's ice shelf. Terminus position is given as distance downstream of the grounding line along the flowline. Surface speeds are compiled from published interferometric SAR (InSAR), SAR speckle tracking and Landsat feature-tracking data (Joughin and others, 2003, 2010; Rignot, 2006, 2008). Where available, terminus speeds are shown for direct comparison with terminus advance rates; these speeds are shown as horizontal gray lines for longer measurement periods on Smith and Thwaites Glaciers and as triangles for shorter measurement periods on Pine Island Glacier. For Crosson Ice Shelf and Thwaites Glacier Tongue, the terminus speed is estimated as its maximum observed value during each study period (Ferrigno and others, 1993; Lucchitta and others, 1994; Rosanova and others, 1998; Rignot, 2001; Lang and others, 2004; Joughin and others, 2009; http://nsidc.org/data/velmap/pine_getz/thwaites/thwaites.html). For Haynes Glacier, the grounding-line speeds shown are the nearest available data along the western edge of Thwaites Glacier, where these two glaciers merge. Vertical gray dashed lines denote the onsets of major rifting events. Linear least-squares terminus advance rates are shown for each sufficiently well-sampled period of steady advance; uncertainties are the standard errors for a least-squares fit.
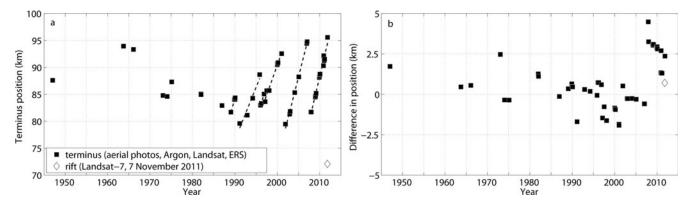
Fig. 4. (a) History of the terminus position of Pine Island Glacier between 1947 and 2011 derived using a 21.5 km wide open-ended box instead of the flowline method shown in Figure 3e. (b) Difference between box- and flowline-derived terminus positions.
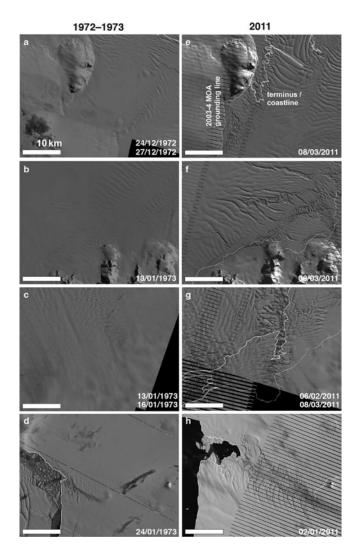

Fig. 5. Pairs of Landsat scenes showing the eastern ASE's marginal ice-shelf changes between 1972 and 2011. (a, e) The Crosson Ice Shelf (northwestern margin); (b, f) Crosson Ice Shelf (southeastern margin); (c, g) Thwaites Glacier Tongue; (d, h) Pine Island Glacier's ice shelf (northern margin). Scene acquisition dates (dd/mm/yyyy) are given in lower right-hand corner of each panel. Note the resolution difference between scenes from 1972–73 (60 m) and 2011 (30 m shown here). The same scale is used for all panels. The striping visible in the 2011 scenes is due to an unrepaired malfunction in the Landsat-7 platform that occurred in 2003.

Although the box method is a better representation of the behaviour of the Pine Island Glacier terminus as a whole, it produced a noisier record whose terminus advance rates do not agree as well with existing surface speed data. This result is consistent with expectations, in that by including more of the terminus in the calculation of its along-flow position, the box method captures more small calving events. The box method is affected more strongly by the limited satellite coverage earlier in our study period, where coastline traces occasionally end abruptly along a terminus of interest (e.g. Animation 1). The compromises required in such cases result in terminus positions derived using the box method that are not directly comparable. We therefore chose to use the simpler flowline method to report terminus histories of the glaciers that we studied (Fig. 3).

COASTAL EVOLUTION

Our terminus histories exhibit sawtooth patterns of steady advance punctuated by periodic calving (Fig. 2). The terminus position along all central flowlines in late 2011 has either retreated or is about to retreat (in the case of Pine Island Glacier) further upstream than compared with late 1972 or early 1973. In addition to this long-term retreat, we observe more rapid, non-periodic terminus retreat along the margins of the ice shelves downstream of all four outlet glaciers. In all cases, marginal rifting precedes this retreat (Fig. 5; Animations 5–7). Below we describe the coastal evolution of each glacier system from west to east.

Smith Glacier is buttressed by Crosson Ice Shelf, which is confined along its northwestern and southeastern margins by Bear Peninsula and Mount Murphy/Haynes Glacier, respectively. Since 1984, Crosson Ice Shelf has progressively rifted and detached from Bear Peninsula both in the vicinity of Holt Glacier (Fig. 5a and e; Animation 5) and further upstream, leading to terminus retreat along that margin. By 2011, the terminus along the northwestern margin was 24 km further upstream than in 1990, and <10 km of the length of the northwestern margin of Crosson Ice Shelf remained attached to Bear Peninsula. Along this ice shelf's opposite margin next to Mount Murphy, rifts elongated, widened and increased in density beginning in 2000. As of late 2011, this rifting is widespread along at least a 28 km long portion of the margin between the terminus and the 2003–04 Moderate Resolution Imaging Spectroradiometer (MODIS) Mosaic of Antarctica (MOA) grounding line along the northeastern flank of Mount

Murphy. In 1972, two ice rises were apparent ~6 km north of the flowline shown in Figure 1 (Lucchitta and others, 1994); the downstream ice rise appears to have ungrounded by 1996 and the effect of the upstream ice rise disappeared after 2007. Our observations of marginal rifting, terminus retreat and ungrounding of Crosson Ice Shelf are coincident with a doubling in speed of Smith Glacier at the grounding line after 1992 (Rignot, 2006, 2008) (Fig. 3a). Some of the highest rates of speed-up on Crosson Ice Shelf between 1996 and 2007–08 ($>500\,\mathrm{m\,a^{-1}}$) are focused at, or upstream of, the marginal rifting and retreat we observed (Rignot, 2008; Fig. 1b).

In 1973, the ice shelf of Haynes Glacier loosely connected Crosson Ice Shelf and Thwaites Glacier Tongue, but it has progressively disintegrated since 1984 (Animation 5) and since 2004 its terminus has remained at or near its grounding line. As a result, any lateral drag that the ice shelf of Haynes Glacier once provided to either of these ice masses has been lost. The 1992–2008 acceleration of the eastern margin of Haynes Glacier (Rignot, 2006, 2008) is contemporaneous with the later stages of its ice shelf's disintegration, but appears to have continued after its terminus stabilized near the grounding line (Fig. 3b), which suggests that driving stress has also increased on Haynes Glacier since 2004. However, the slowdown across its central trunk between 1996 and 2007–08 (Rignot, 2008; Fig. 1b) and the lower rate of its most recent terminus advance suggest that much of the response of its central trunk to ice-shelf disintegration occurred before 1996.

Where Thwaites Glacier goes afloat, it forms two distinct floating ice masses: (1) Thwaites Glacier Tongue, which is downstream of the central area of fastest flow; and (2) the eastern ice shelf, which extends east of the ice tongue and was partially connected to it until 2010 (Fig. 5c and g; Animation 6). A pinning point ~45 km downstream of the eastern ice shelf's grounding line restricts its flow (Rignot, 2001; Tinto and Bell, 2011), causing deceleration between its grounding line and terminus (Fig. 3d) and inducing shear between the ice tongue and ice shelf. The floating ice between these two ice masses originates where a major shear zone emerges from Thwaites Glacier (Rignot, 2001, 2006) and is an area of recent acceleration (Rignot, 2008; Fig. 1b). Rapid upstream propagation of the terminus in this narrow region began in 2009 and the terminus is now 26 km further upstream than in 1973 and is within ~4 km of the grounding line. After 1989, transverse-to-flow rifts grew in size and density near the grounding line of Thwaites Glacier, particularly along its western flank (e.g. Rignot, 2001); similar rifts appeared near the grounding line of the eastern ice shelf in 2001 (Rignot, 2006). In 2010, Thwaites Glacier Tongue calved within 16 km of the grounding line, although the new ~$2240\,\mathrm{km^2}$ iceberg and the smaller remaining ice tongue are presently still connected by an ice melange. Thwaites Glacier Tongue is not believed to buttress Thwaites Glacier significantly (Rignot, 2001), which is consistent with the muted recent acceleration of the grounded ice directly upstream of the ice tongue (up to 16% between 1992 and 2007; Rignot, 2006, 2008; Fig. 3c) compared with other glaciers in the ASE (63–108% over the same period), despite similar observations of marginal rifting and terminus retreat. The terminus advance rate did not change significantly after the 2010 calving event, which removed most of the remaining ice tongue; this observation supports the earlier calculations of its limited buttressing effect.

Pine Island Glacier is buttressed by an ice shelf whose flow is resisted primarily by shear along the adjacent slower-flowing southern and northern ice shelves (Rignot, 2002; Schmeltz and others, 2002). An ice rise that existed prior to 1982 formerly provided additional resistance to flow (Jenkins and others, 2010). The northern shear margin of this ice shelf has progressively rifted apart since 1997 (Bindschadler, 2002), and rifts now extend along a 21 km long zone from the 2011 terminus to the grounding line (Fig. 5d and h; Animation 7). This rifting originates at two ice rises (Bindschadler, 2002); since 2002 the downstream ice rise no longer clearly generates rifts, suggesting that the ice shelf has progressively ungrounded there. Consequently, since 2008 the terminus has retreated across this narrow rifted zone. A loss of buttressing along the northern margin has been predicted to result in a 20% increase in terminus speed (Schmeltz and others, 2002), so rifting alone cannot explain the observed ~60% terminus acceleration between 1996 and 2010 (Joughin and others, 2003, 2010; Rignot, 2006, 2008) (Fig. 3e) that models have suggested is due primarily to ungrounding of an ice plain (e.g. Thomas and others, 2004b). The southern margin of the ice shelf has retreated similarly, although the ice there is much less fractured near its terminus, which is consistent with observed greater acceleration along the northern margin of the ice shelf relative to its southern margin (Rignot, 2008; Fig. 1c). Rifting along the southern shear margin 40–60 km upstream of the terminus began in 1999. The difference in degree of fracturing between the northern and southern shear margins is presumably due to the lack of ice rises along the southern margin (Rignot, 2002).

DISCUSSION

Ice flux across the grounding line is less sensitive to ice-shelf buttressing than it is to ice thickness there (Schoof, 2007), hence most recent studies of floating ice in the eastern ASE have focused on the pattern of sub-ice-shelf melting (Jenkins and others, 2010; Jacobs and others, 2011) and its role in grounding-line ice dynamics (Joughin and others, 2010). Our observations indicate that ice-shelf marginal rifting and terminus retreat along these rifted margins were widespread in the eastern ASE between 1972 and 2011, particularly beginning in the late 1990s. Ice melange within these rifts is expected to support much less force transmission between opposing rift faces than would have existed prior to rift formation (MacAyeal and others, 1998). Therefore, these changes must have reduced the lateral drag of the ice shelves, although ice-flow acceleration and spatially varying thinning may have partially counterbalanced their effect by increasing lateral drag. The spatio-temporal resolutions of ice-flow speed and ice-shelf thinning histories during our study period preclude quantification of buttressing loss in the eastern ASE, or a conclusive apportionment of this buttressing loss between ice-shelf thinning and margin disintegration. However, reported accelerations are generally contemporaneous and spatially coherent with these marginal changes, strongly suggesting that this pattern of coastal change also reduced buttressing and contributed to acceleration of upstream grounded ice.

A sequence of ice-shelf thinning, acceleration, marginal rifting and disintegration was proposed to explain the 1998–2003 acceleration of Jakobshavn Isbræ, Greenland (Joughin and others, 2008). The major outlet glaciers of the eastern

ASE have recently undergone elements of this same sequence, although only Haynes Glacier's ice shelf has completely disintegrated so far. This acceleration was likely initiated by two mechanisms: (1) redistribution of driving stress towards the grounding line due to enhanced sub-ice-shelf melting near there (Schoof, 2007); or (2) decreased ice-shelf buttressing due to loss of basal and lateral drag as thinning ice shelves ungrounded from ice rises and reduced their contact area with side walls. We hypothesize that the development and growth of marginal rifts is favoured during periods of ice-shelf thinning and outlet glacier acceleration. Thus, the accelerations of these glaciers have apparently led to an additional form of buttressing loss: decreased ice-shelf lateral drag due to marginal rifting. Continued acceleration should lead to further rifting, potentially creating a feedback until all lateral resistance to ice-shelf flow is lost.

We hypothesize that rifting is favoured along the ice-shelf margins because these regions were once shear margins within grounded ice further upstream (Fig. 1). Shear margins are expected to be rheologically weaker (Echelmeyer and others, 1994; MacAyeal and others, 1998; Khazendar and others, 2007) and have numerous surface crevasses that may connect with basal crevasses forming at the grounding line to create rifts (Catania and others, 2006). Ice-shelf thinning promotes basal crevasse growth (Van der Veen, 1998) and is widespread in the ASE (e.g. Schmeltz and others, 2001; Zwally and others, 2005; Jenkins and others, 2010), so the marginal rifting we report may not be due solely to acceleration or pre-existing weakness.

This slower style of ice-shelf disintegration and the hypothesized underlying mechanisms are distinct from the much faster (multi-day) catastrophic disintegrations of the Larsen A/B and Wilkins ice shelves in the Antarctic Peninsula, which are believed to have been induced by surface-meltwater-enhanced fracture propagation and ice-berg capsizing (Scambos and others, 2000, 2009; MacAyeal and others, 2003). However, pre-existing rifts may also have weakened those ice shelves and influenced the extent of those faster disintegrations (e.g. Khazendar and others, 2007). We speculate that margin-led rifting is a common feature in the non-catastrophic break-up of thicker ice shelves since it seems to occur whenever these ice shelves accelerate significantly relative to their margins. Such acceleration can originate in several different ways, and ice-shelf margins are often zones of inherited weakness. Jakobsson and others (2011) proposed that the late-Pleistocene collapse of a large ice shelf in the present-day Amundsen Sea was initiated by rapid sea-level rise and involved grounding-line rifting. Both marginal and grounding-line rifting are occurring presently in the ASE (e.g. Thwaites Glacier) and the former generally precedes the latter, so marginal rifting may also have played a role in the late-Pleistocene event.

OUTLOOK

Along with the potential continuation of enhanced Circumpolar Deep Water delivery into the ASE (Steig and others, 2012), which would lead to further sub-ice-shelf melting, several observations of the present configuration of floating ice in the eastern ASE suggest that reductions in buttressing will continue. First, since 2000, large transverse rifts across Crosson Ice Shelf have begun to propagate from the southeast and now extend across two-thirds of its width. If these rifts continue to grow, its downstream half will calve off and its terminus will be further upstream than at any other time since 1972. Second, if the eastern ice shelf of Thwaites Glacier calves in the vicinity of transverse rifts near its grounding line, as Thwaites Glacier Tongue did in 2010, the buttressing currently provided by the pinning point at its terminus will be lost (Rignot, 2006). Third, if terminus retreat along the southern margin of Pine Island Glacier's ice shelf continues, its southwestern tributary will lose any buttressing provided by direct contact with the southern ice shelf. The rift that developed in late 2011 across Pine Island Glacier's ice shelf is further upstream than any previously observed terminus position, including its first sighting in 1947 (Rignot, 2002; Howat and others, 2012; Figs 1 and 4a). However, it does not appear that the calving of this portion of the ice shelf will result in any substantial additional buttressing loss, due to pre-existing marginal rifts. Rifting often occurs in the lee of ice rises and can destabilize ice-shelf flow (e.g. Doake and Vaughan, 1991), but as ice shelves thin they also unground from ice rises and no longer generate rifts, so any further rifting in the eastern ASE will likely nucleate at ice-shelf margins or the grounding line (e.g. Thwaites Glacier).

Two modelling challenges that arise from our observations are the accurate portrayal of the style of progressive margin-led ice-shelf disintegration that we observe throughout the eastern ASE, and evaluation of its potential feedback with outlet glacier acceleration. So far, this style of buttressing loss has only been simulated in this region for Pine Island Glacier by instantaneously removing portions of its ice shelf (Schmeltz and others, 2002; Joughin and others, 2010). The effect of rifts upon the flow of the Filchner–Ronne Ice Shelf has been simulated successfully using diagnostic finite-element modelling (e.g. MacAyeal and others, 1998), but additional work is necessary to include marginal rifting and its effects in predictive ice-sheet models. This work should include both field and remote-sensing studies of the internal glacier stresses that likely dominate marginal rift evolution (e.g. Bassis and others, 2008) and modelling studies of the effect of marginal rifting upon ice-flow evolution (e.g. Vieli and Nick, 2011). Accurate modelling of calving rates is another outstanding challenge in glaciology (Alley and others, 2008), and prediction of calving in the eastern ASE using ice-flow models can be improved using the histories of terminus position presented here.

REFERENCES

Alley RB and 7 others (2008) A simple law for ice-shelf calving. *Science,* **322**(5906), 1344 (doi: 10.1126/science.1162543)

Bassis JN, Fricker HA, Coleman R and Minster J-B (2008) An investigation into the forces that drive ice-shelf rift propagation on the Amery Ice Shelf, East Antarctica. *J. Glaciol.,* **54**(184), 17–27 (doi: 10.3189/002214308784409116)

Bindschadler RA (2002) History of lower Pine Island Glacier, West Antarctica, from Landsat imagery. *J. Glaciol.,* **48**(163), 536–544 (doi: 10.3189/172756502781831052)

Catania GA, Conway H, Raymond CF and Scambos TA (2006) Evidence for floatation or near floatation in the mouth of Kamb Ice Stream, West Antarctica, prior to stagnation. *J. Geophys. Res.,* **111**(F1), F01005 (doi: 10.1029/2005JF000355)

Chen JL, Wilson CR, Blankenship D and Tapley BD (2009) Accelerated Antarctic ice loss from satellite gravity measurements. *Nature Geosci.,* **2**(12), 859–862 (doi: 10.1038/ngeo694)

Doake CSM and Vaughan DG (1991) Rapid disintegration of the Wordie Ice Shelf in response to atmospheric warming. *Nature,* **350**(6316), 328–330

Echelmeyer KA, Harrison WD, Larsen C and Mitchell JE (1994) The role of the margins in the dynamics of an active ice stream. *J. Glaciol.,* **40**(136), 527–538

Ferrigno JG, Lucchitta BK, Mullins KF, Allison AL, Allen RJ and Gould WG (1993) Velocity measurements and changes in position of Thwaites Glacier/iceberg tongue from aerial photography, Landsat images and NOAA AVHRR data. *Ann. Glaciol.,* **17**, 239–244

Holt JW and 8 others (2006) New boundary conditions for the West Antarctic Ice Sheet: subglacial topography of the Thwaites and Smith glacier catchments. *Geophys. Res. Lett.,* **33**(9), L09502 (doi: 10.1029/2005GL025561)

Howat IM and 8 others (2012) Rift in Antarctic glacier: a unique chance to study ice shelf retreat. *Eos,* **93**(8), 77–88

Jacobs SS, Jenkins A, Giulivi CF and Dutrieux P (2011) Stronger ocean circulation and increased melting under Pine Island Glacier ice shelf. *Nature Geosci.,* **4**(8), 519–523 (doi: 10.1038/ngeo1188)

Jakobsson M and 15 others (2011) Geological record of ice shelf break-up and grounding line retreat, Pine Island Bay, West Antarctica. *Geology,* **39**(7), 691–694 (doi: 10.1130/G32153.1)

Jenkins A and 6 others (2010) Observations beneath Pine Island Glacier in West Antarctica and implications for its retreat. *Nature Geosci.,* **3**(7), 468–472 (doi: 10.1038/ngeo890)

Joughin I, Rignot E, Rosanova CE, Lucchitta BK and Bohlander J (2003) Timing of recent accelerations of Pine Island Glacier, Antarctica. *Geophys. Res. Lett.,* **30**(13), 1706 (doi: 10.1029/2003GL017609)

Joughin I and 7 others (2008) Continued evolution of Jakobshavn Isbræ following its rapid speedup. *J. Geophys. Res.,* **113**(F4), F04006 (doi: 10.1029/2008JF001023)

Joughin I and 6 others (2009) Basal conditions for Pine Island and Thwaites Glaciers, West Antarctica, determined using satellite and airborne data. *J. Glaciol.,* **55**(190), 245–257 (doi: 10.3189/002214309788608705)

Joughin I, Smith BE and Holland DM (2010) Sensitivity of 21st century sea level to ocean-induced thinning of Pine Island Glacier, Antarctica. *Geophys. Res. Lett.,* **37**(20), L20502 (doi: 10.1029/2010GL044819)

Khazendar A, Rignot E and Larour E (2007) Larsen B Ice Shelf rheology preceding its disintegration inferred by a control method. *Geophys. Res. Lett.,* **34**(19), L19503 (doi: 10.1029/2007GL030980)

Kim K, Jezek KC and Liu H (2007) Orthorectified image mosaic of Antarctica from 1963 Argon satellite photography: image processing and glaciological applications. *Int. J. Remote Sens.,* **28**(23), 5357–5373 (doi: 10.1080/01431160601105850)

Lang O, Rabus BT and Dech SW (2004) Velocity map of the Thwaites Glacier catchment, West Antarctica. *J. Glaciol.,* **50**(168), 46–56 (doi: 10.3189/172756504781830268)

Lemke P and 10 others (2007) Observations: changes in snow, ice and frozen ground. In Solomon S and 7 others eds. *Climate change 2007: the physical science basis. Contribution of Working Group I to the Fourth Assessment Report of the Intergovernmental Panel on Climate Change.* Cambridge University Press, Cambridge, 339–383

Lucchitta BK, Mullins KF, Smith CE and Ferrigno JG (1994) Velocities of the Smith Glacier ice tongue and Dotson Ice Shelf, Walgreen Coast, Marie Byrd Land, West Antarctica. *Ann. Glaciol.,* **20**, 101–109

MacAyeal DR, Rignot E and Hulbe CL (1998) Ice-shelf dynamics near the front of the Filchner–Ronne Ice Shelf, Antarctica, revealed by SAR interferometry: model/interferogram comparison. *J. Glaciol.,* **44**(147), 419–428

MacAyeal DR, Scambos TA, Hulbe CL and Fahnestock MA (2003) Catastrophic ice-shelf break-up by an ice-shelf-fragment-capsize mechanism. *J. Glaciol.,* **49**(164), 22–36 (doi: 10.3189/172756503781830863)

Moon T and Joughin I (2008) Changes in ice front position on Greenland's outlet glaciers from 1992 to 2007. *J. Geophys. Res.,* **113**(F2), F02022 (doi: 10.1029/2007JF000927)

Pritchard HD, Arthern RJ, Vaughan DG and Edwards LA (2009) Extensive dynamic thinning on the margins of the Greenland and Antarctic ice sheets. *Nature,* **461**(7266), 971–975 (doi: 10.1038/nature08471)

Rignot E (2001) Evidence for rapid retreat and mass loss of Thwaites Glacier, West Antarctica. *J. Glaciol.,* **47**(157), 213–222 (doi: 10.3189/172756501781832340)

Rignot E (2002) Ice-shelf changes in Pine Island Bay, Antarctica, 1947–2000. *J. Glaciol.,* **48**(161), 247–256 (doi: 10.3189/172756502781831386)

Rignot E (2006) Changes in ice dynamics and mass balance of the Antarctic ice sheet. *Philos. Trans. R. Soc. London, Ser. A,* **364**(1844), 1637–1655

Rignot E (2008) Changes in West Antarctic ice stream dynamics observed with ALOS PALSAR data. *Geophys. Res. Lett.,* **35**(12), L12505 (doi: 10.1029/2008GL033365)

Rignot E, Mouginot J and Scheuchl B (2011) Ice flow of the Antarctic Ice Sheet. *Science,* **333**(6048), 1427–1430 (doi: 10.1126/science.1208336)

Rosanova CE, Lucchitta BK and Ferrigno JG (1998) Velocities of Thwaites Glacier and smaller glaciers along the Marie Byrd Land coast, West Antarctica. *Ann. Glaciol.,* **27**, 47–53

Scambos TA, Hulbe C, Fahnestock M and Bohlander J (2000) The link between climate warming and break-up of ice shelves in the Antarctic Peninsula. *J. Glaciol.,* **46**(154), 516–530 (doi: 10.3189/172756500781833043)

Scambos TA, Haran TM, Fahnestock MA, Painter TH and Bohlander J (2007) MODIS-based Mosaic of Antarctica (MOA) data sets: continent-wide surface morphology and snow grain size. *Remote Sens. Environ.,* **111**(2–3), 242–257 (doi: 10.1016/j.rse.2006.12.020)

Scambos T and 7 others (2009) Ice shelf disintegration by plate bending and hydro-fracture: satellite observations and model results of the 2008 Wilkins ice shelf break-ups. *Earth Planet. Sci. Lett.,* **280**(1–4), 51–60 (doi: 10.1016/j.epsl.20082.027)

Schmeltz M, Rignot E and MacAyeal DR (2001) Ephemeral grounding as a signal of ice-shelf change. *J. Glaciol.,* **47**(156), 71–77 (doi: 10.3189/172756501781832502)

Schmeltz M, Rignot E, Dupont TK and MacAyeal DR (2002) Sensitivity of Pine Island Glacier, West Antarctica, to changes in ice-shelf and basal conditions: a model study. *J. Glaciol.,* **48**(163), 552–558 (doi: 10.3189/172756502781831061)

Schoof C (2007) Ice sheet grounding line dynamics: steady states, stability, and hysteresis. *J. Geophys. Res.,* **112**(F3), F03S28 (doi: 10.1029/2006JF000664)

Shepherd A, Wingham D and Mansley JA (2002) Inland thinning of the Amundsen Sea sector, West Antarctica. *Geophys. Res. Lett.,* **29**(10), 1364 (doi: 10.1029/2001GL014183)

Steig EJ, Ding Q, Battisti DS and Jenkins A (2012) Tropical forcing of Circumpolar Deep Water inflow and outlet glacier thinning in the Amundsen Sea Embayment, West Antarctica. *Ann. Glaciol.,* **53**(60), 19–28 (doi: 10.3189/2012AoG60A110)

Swithinbank C, Williams RS, Jr, Ferrigno JG, Foley KM and Rosanova CE (2003) Coastal-change and glaciological map of the Bakutis Coast area, Antarctica: 1972–2002. *USGS Geol. Invest. Map* I-2600-F

Swithinbank C, Williams RS, Jr, Ferrigno JG, Foley KM, Rosanova CE and Dailide LM (2004) Coastal-change and glaciological map of the Eights Coast area, Antarctica: 1972–2001. *USGS Geol. Invest. Map* I-2600-E

Thomas R and 17 others (2004a) Accelerated sea-level rise from West Antarctica. *Science,* **306**(5694), 255–258

Thomas RH, Rignot EJ, Kanagaratnam K, Krabill WB and Casassa G (2004b) Force-perturbation analysis of Pine Island Glacier, Antarctica, suggests cause for recent acceleration. *Ann. Glaciol.,* **39**, 133–138 (doi: 10.3189/172756404781814429)

Tinto KJ and Bell RE (2011) Progressive unpinning of Thwaites Glacier from newly identified offshore ridge: constraints from aerogravity. *Geophys. Res. Lett.,* **38**(20), L20503 (doi: 10.1029/2011GL049026)

Van der Veen CJ (1998) Fracture mechanics approach to penetration of bottom crevasses on glaciers. *Cold Reg. Sci. Technol.,* **27**(3), 213–223 (doi: 10.1016/S0165-232X(98)00006-8)

Vaughan DG and 9 others (2006) New boundary conditions for the West Antarctic ice sheet: subglacial topography beneath Pine Island Glacier. *Geophys. Res. Lett.,* **33**(9), L09501 (doi: 10.1029/2005GL025588)

Vieli A and Nick FM (2011) Understanding and modelling rapid dynamic changes of tidewater outlet glaciers: issues and implications. *Surv. Geophys.,* **32**(4–5), 437–458 (doi: 10.1007/s10712-011-9132-4)

Zwally HJ and 7 others (2005) Mass changes of the Greenland and Antarctic ice sheets and shelves and contributions to sea-level rise: 1992–2002. *J. Glaciol.,* **51**(175), 509–527 (doi: 10.3189/172756505781829007)